

X-ray crystal structures of a severely desiccated protein

JEFFREY A. BELL

Division of Molecular Medicine, Wadsworth Center, New York State Department of Health,
P.O. Box 509, Empire State Plaza, Albany, New York 12201-0509

(RECEIVED May 17, 1999; ACCEPTED July 30, 1999)

Abstract

Unlike most protein crystals, form IX of bovine pancreatic ribonuclease A diffracts well when severely dehydrated. Crystal structures have been solved after 2.5 and 4 days of desiccation with CaSO_4 , at 1.9 and 2.0 Å resolution, respectively. The two desiccated structures are very similar. An RMS displacement of 1.6 Å is observed for main-chain atoms in each structure when compared to the hydrated crystal structure with some large rearrangements observed in loop regions. The structural changes are the result of intermolecular contacts formed by strong electrostatic interactions in the absence of a high dielectric medium. The electron density is very diffuse for some surface loops, consistent with a very disordered structure. This disorder is related to the conformational changes. These results help explain conformational changes during the lyophilization of protein and the associated phenomena of denaturation and molecular memory.

Keywords: dehydration; dielectric constant; disulfide bonds; electrostatic interactions; lyophilization; protein conformation; water

Crystal form IX of ribonuclease A was discovered by David Harker and coworkers (King et al., 1962). When completely solvated, the structure of ribonuclease in this crystal form is typical of that found in eight other crystal environments (Dung & Bell, 1997). This crystal form is rather densely packed, but not exceptionally so (1.94 Å³/Da, 30% solvent by volume; Matthews, 1968). It is noteworthy due to its ability to withstand severe desiccation and still diffract X-rays at high resolution.

The structure of a desiccated protein is more than a curiosity. Knowledge of dehydrated protein structure is important because pharmaceutical proteins are formulated as lyophilized powders and because rehydration without loss of activity to denaturation can be difficult to achieve (Carpenter et al., 1997; Costantino et al., 1998). In addition, a structural basis is still being developed for the phenomenon of molecular memory, whereby the presence of a bound ligand during lyophilization determines activity characteristics of the protein when it is subsequently suspended in nonaqueous solvent (Mishra et al., 1996). More fundamentally, computing the influence of water interactions on protein structure is an important issue (Hartsough & Merz, 1992; Steinbach & Brooks, 1993; Zheng & Ornstein, 1996) that may benefit from additional experimental data.

Most of the observed changes in protein properties with dehydration, as detected by NMR relaxation times, heat capacity, and

dielectric behavior, have occurred before hydration levels decrease to 0.05 g H₂O/g protein (Rupley & Careri, 1991). (1 g/g corresponds to approximately 6 water molecules per residue.) Infrared spectroscopy, especially, has produced some intriguing results regarding protein structural changes at these low levels of hydration. Upon lyophilization, the secondary structure content of most protein powders, including bovine pancreatic ribonuclease A, changes markedly, with an apparent decrease in helical content, an apparent increase in beta sheet, and usually a decrease in "less ordered" structures (Griebenow & Klivanov, 1995; Dong et al., 1996). The magnitude of the change is highly dependent on solution conditions during lyophilization for some proteins (Desai et al., 1994; Desai & Klivanov, 1995; Prestrelski et al., 1995), but not for others (Costantino et al., 1995). For hen egg white lysozyme (HEWL), the most intensely studied protein with respect to dehydration, spectroscopic indications of conformational changes start at 0.22 g/g and are complete by 0.1 g/g (Rupley & Careri, 1991; Poole, 1994).

At levels of hydration less than 0.2 g/g, protein mobility reaches a minimum that does not change much with further dehydration (Rupley & Careri, 1991). For some proteins such as lysozyme and human serum albumin, but not others such as bovine serum albumin, further dehydration increases the number of conformational states sampled (Gregory et al., 1993; Shah & Ludescher, 1993). In this respect, dehydrated proteins have been characterized as having glass-like properties. This dehydration phenomenon has been linked to the transition in hydrated protein dynamic properties below 220 K, which is characterized by the adoption of many individual conformational substates that do not interconvert (Rupley & Careri, 1991).

Reprint requests to: Jeffrey A. Bell, Division of Molecular Medicine, Wadsworth Center, New York State Department of Health, P.O. Box 509, Empire State Plaza, Albany, New York 12201-0509; e-mail: bell@wadsworth.org.

Crystallography has already provided some insight into the dehydration process, mostly from extensive investigations of HEWL. At the lowest level of hydration previously examined for an uncross-linked protein crystal, lysozyme was analyzed at a relative humidity of 5%, which corresponds to a water vapor pressure of ~ 1 Torr at room temperature (Nagendra et al., 1998). Twenty-three water molecules were observed in the electron density for each protein molecule. The water content of these crystals was less than 0.08 g/g, under which conditions any conformational changes in lysozyme would have been completed in the powder (Poole, 1994). Although no overt conversion of secondary structure was observed, domain motions and changes in loop structure were observed, producing RMS differences in alpha carbon positions of 1.0 Å. At this level of hydration, glass-like behavior would not be expected. In another study using crystals with intermolecular cross-linking, lysozyme crystals were examined by X-ray diffraction after dehydration over silica gel. A brief report described an RMS deviation (RMSD) for main-chain atoms of 0.6 Å from their positions in the solvated structure (Kachalova et al., 1991).

Ribonuclease A crystals (space group $P2_1$) have been analyzed after very limited dehydration at a relative humidity of 79%. Coordinates were determined for 145 water molecules per protein, and small changes in structure (variation in alpha carbon position of 0.5 Å RMS) were observed (Radha Kishan et al., 1995).

Several important questions about protein dehydration remain active topics for research, which crystallographic analysis could help answer. Especially intriguing is the nature and cause of the dehydration-induced conformational changes indicated by spectroscopic techniques. Also not fully explained is the reason that a protein would become glass-like upon dehydration.

Results

The desiccated structures

The crystal structure of bovine pancreatic ribonuclease A form IX was determined after both 2.5 and 4 days of dehydration with CaSO_4 (Bell, 1997). The drying procedure (relative humidity less than 0.03%, water concentration approximately 5×10^{-3} Torr; Shriver & Drezdson, 1969) resulted in a reduction of the unit cell volume (Bell, 1997), to produce the second most densely packed protein crystals yet reported (Nagendra et al., 1998). The Matthews coefficient of the desiccated crystals was $1.30 \text{ \AA}^3/\text{Da}$ with only 10% volume unoccupied by protein or counterions. The decrease in the size of the unit cell sometimes led to cracks or breaks in the crystal, depending on surface adhesion. Diffraction maxima had a larger mosaic spread after drying. Nevertheless, the crystals remained well enough ordered to produce 1.9 Å reflections.

Differences between the two desiccated structures are slight, both in terms of structure (Fig. 1A) and thermal parameters (Fig. 1B). The largest difference in the coordinates occurs near residue 89 (Fig. 1A), a region of high thermal parameters in which the orientation of the carbonyl is reversed or "flipped" between the two structures. This difference appears real, as judged by the effects on R_{free} (R -factor computed using a small portion of the data not employed in the refinement; Brünger, 1992) when the alternate conformation was assessed in each structure. Both conformations are likely to be present in each structure, but in different proportions. The close agreement between the two structures demonstrates that the structural results may be obtained reproducibly from the desiccation procedure.

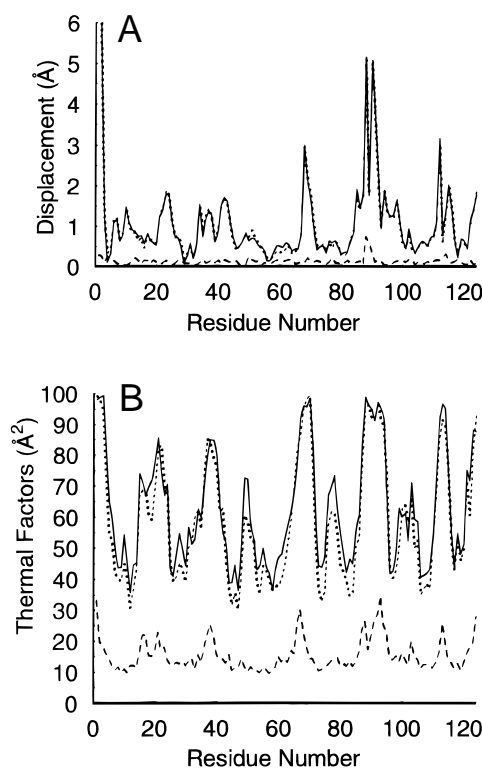


Fig. 1. A: The deviation of alpha carbon atom positions after superposition (Tronrud et al., 1987) for all pairings of the two dehydrated and one hydrated structures, plotted vs. residue number. The differences in the two desiccated structures (---) are very small, with an RMSD of 0.29 Å for main-chain atoms. The magnitude of the displacements for the 2.5 day (···) and 4 day (—) desiccated structures from the hydrated structure are much larger, resulting in RMSDs of 1.58 and 1.56 Å, respectively, for main-chain atoms. Values comparing the desiccated and hydrated structures at residue 1 are truncated. **B:** The average main-chain thermal factors plotted vs. residue number. The 2.5 day desiccated structure (···) and the 4 day desiccated structure (—) have very similar thermal factors (correlation = 0.97). Although always lower, the thermal factors for the hydrated structure (---) are correlated with those of the desiccated structures (correlation of 0.80 and 0.78 for the 2.5 and 4 day desiccated structures, respectively). This figure was prepared using the program Axum (MathSoft).

Figure 2 illustrates the quality of the electron density map for the 2.5 day desiccated structure, from one of the better resolved residues, phenylalanine 46, to some weaker electron density near serine 50. The effect of disorder on the electron density map may be observed by following how well the carbonyl oxygens are resolved as one moves down the polypeptide chain from a region of relatively low thermal factors to residues with much higher ones (Fig. 1B).

Continuous electron density is observed at the 1σ contour level for the main-chain atoms, except for the chain termini and residues 15, 37, 69–70, 90–92, and 111. External side chains are usually represented by diffuse electron density, unless they are involved in specific interactions, especially with counterions, as described below.

Clearly resolved in the desiccated structures are three sulfate ions, which mediate many intermolecular contacts in the crystal (Table 1). Sulfate ions 151 and 152 (Fig. 3A) are notable for being very close together, bridged by the epsilon amino group of lysine 31. In addition, lysines 7 and 41, and histidines 12 and 119, are within van der Waals contact of these two sulfates. Three different

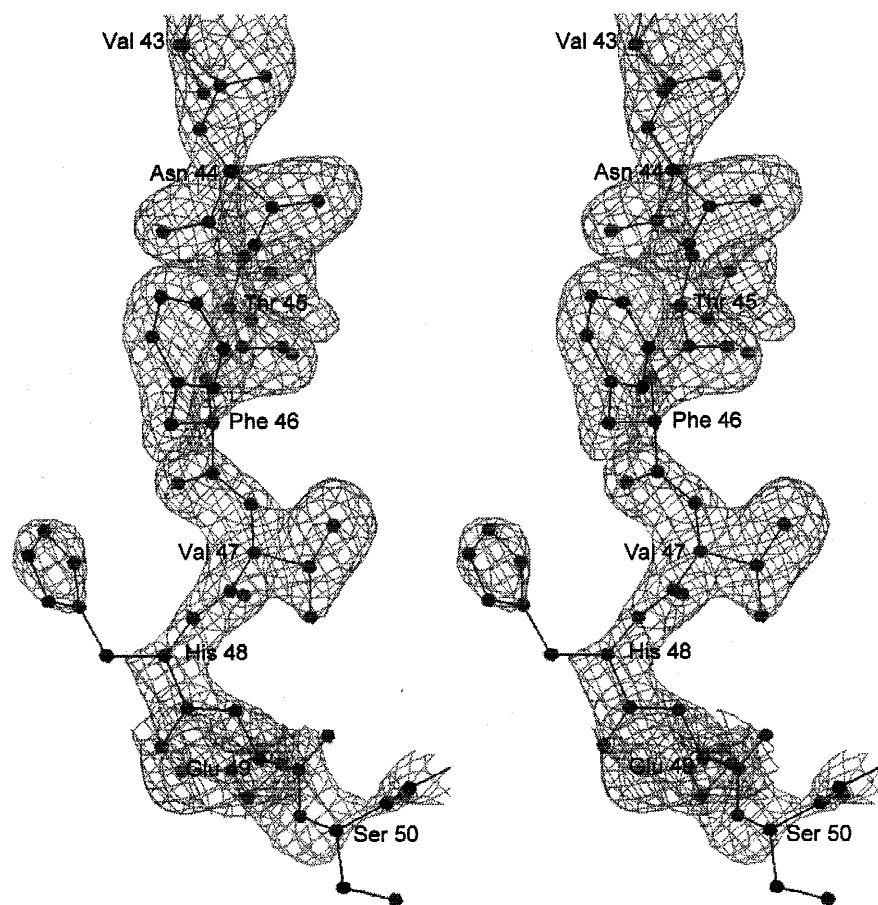


Fig. 2. Stereodiamgram showing the electron density map ($2F_o - F_c$) contoured at the 1σ level for residues 43 to 50 in the 2.5 day desiccated structure. None of the residues shown were included in the model for calculation of this electron density map. The gradient of thermal factors along this stretch of beta sheet is very high (Fig. 1). This figure was prepared using the program SETOR (Evans, 1993).

symmetry-related molecules contribute the above residues to this charge cluster.

Sulfate 150 is also involved in multiple intermolecular interactions. It is situated at the N-terminal end of the helix composed of residues 51 to 58. It forms hydrogen bonds with lysine 91 from one symmetry-related molecule and with lysine 61 from another symmetry-related molecule. In total, residues from four different protein molecules make contact with sulfate 150 (Fig. 3B).

The electron density map for the 4 day desiccated structure contains evidence of two water molecules. Water 201 is coordinated by sulfate 151, lysine 7, and histidine 119, plus proline 93 from another molecule (Fig. 3A). Water 202 is associated with aspartic acid 53 (Fig. 3B). Comparable electron density is not found in the 2.5 day desiccated structure, contrary to what one might expect from a shorter desiccation period. However, the difference electron density calculated from the observed coefficients and model phases (not shown) confirmed this result.

The presence of water in the 4 day desiccated structure is easily explained if the vapor pressure of water in that case was slightly higher than for the 2.5 day desiccated crystal, due to slight hydration of the desiccant during the mounting and sealing process. This observation is fortuitous in that it provides enough information to conclude that the two most tightly bound water molecules ob-

served in these ribonuclease crystals have a K_d near 5×10^{-3} Torr. The presence of water at these particular sites is consistent with the observation that charged residues within a protein are the most difficult to dehydrate (Rupley & Careri, 1991).

The question of how much total water actually remained in these desiccated protein crystals is not an easy one to answer. From measurements of the water content of ribonuclease powders, one would expect at least four water molecules to be present for each protein (Almog & Schrier, 1978). The volume of the unit cell not occupied by protein or counter ions is $7,460 \text{ \AA}^3$, adequate to contain a maximum of 62 water molecules per protein at the density of bulk water. The refinement parameter K_{sol} , which indicates the ratio of the electron density in solvent regions to that in the protein (Tronrud, 1995), converged to values of 0.68 and 0.59 for the 2.5 and 4.0 day desiccated structures, respectively. These numbers are just below the electron density expected for a low-salt aqueous solvent and indicate that a significant amount of electron density is not explained by the atomic coordinates. This electron density could be attributed to very disordered water, but some or all of it may be due to very disordered side chains not well modeled by a single conformation. Regardless of the value of K_{sol} , one point is clear: the solvent electron density peaks typically found in hydrated structures, and even other rather strongly dehydrated struc-

Table 1. Residues involved in lattice contacts in desiccated crystal structure^a

Interface	Residues molecule 1	Residues molecule 2	Notes on interface
1	1–3	18–19	Similar to solvated structure Also includes sulfates 150 and 152
	5–7	48–53	
	9–10	55–57	
	13–16	59–61	
	28–29	75–80	
	31–34	103	
	37	113–115	
	51		
	55		
2	61–66	19–22	Similar to solvated structure
	69	78	
	74–77	99–104	
	105	123–124	
	107		
	121–122		
	124		
3	1–4	14–25	Similar to solvated structure Also includes sulfates 150 and 151
	7	27–29	
	10–12	31	
	33–41	33	
	65–72	36–38	
	91–92	87–90	
	109	92–96	
	111		
	118–120		
	127		
4	1–2	12	Similar to solvated structure Also includes sulfates 151 and 152
	58–64	39	
	69–71	41–45	
	73	66	
	76	85–91	
	110–116	119–124	
5	83	90–92	Not found in solvated structure
	85–87		
	98–100		
6	17–21	67–69	Not found in solvated structure
	7		
7	21–24	15–18	Not found in solvated structure Also includes sulfate 150
	87–88	50–52	
	97–99		
8	2	68–69	Not found in solvated structure

^aAll contacts generated by a given symmetry relationship are classified together as a single interface. Residues are included in the interface if any atom in the residue was less than 5 Å from another molecule.

tures (Nagendra et al., 1998), were not observed here, except for the two water molecules already described.

Hydrated vs. desiccated structures

Figure 4 shows the two desiccated structures, overlaid on the hydrated structure. The desiccated structures are almost indistinguishable on the scale of this drawing. The largest difference due to desiccation involves the loop between residues 85 and 96, which

connect two adjacent strands of beta sheet. The disulfide bridge between residues 40 and 95 adopts an entirely different conformation between hydrated and desiccated structures. Other loops significantly rearranged in the desiccated structure are also apparent in Figure 4, especially those composed of residues 20 to 25, 66 to 71, and 111 to 117.

The four disulfides in ribonuclease apparently help constrain or reduce the structural distortion that might otherwise occur. For the 85–94 loop, the 26–84 disulfide dampens out the propagation of the effect beyond residue 84, and the 40–95 disulfide serves the same purpose at the other end of this loop. A similar case could be made for the effect of disulfide bonds on conformational changes seen near loops 20–25, 66–71, and 111–117 (Fig. 4).

Thermal factors tend to be distributed in the same manner in either the hydrated or desiccated structures, with the lowest values found for internal protein residues (Fig. 1B). However, the thermal parameters for some of the surface loops of the desiccated structures are very high relative to the hydrated ribonuclease structure. Cysteine residues are all located in or near regions of the structure where the thermal factors change rapidly along the polypeptide chain (Figs. 1, 4). Thus, the disulfide bonds are also seen to help reduce the disordering effect of dehydration within the protein.

The four different interfaces from the solvated structure are similar to the four most extensive sets of interactions in the desiccated structures (Tables 1, 3 of Dung & Bell, 1997). Changes that do occur in these interfaces involve an increase in the number of intermolecular contacts in the desiccated structure. In addition, four new interfaces are formed in the densely packed desiccated structures. Of these latter four, interface 7 is most substantial, and involves a denser packing in the volume surrounding sulfate 150, of contacts already tenuously present in the hydrated structure.

Figure 5 indicates that several residues in the structure are in strained conformations in the desiccated state. These regions of the protein are also where large conformational changes and high thermal factors were observed (Fig. 1). The confluence of these effects of desiccation at the same sites is noteworthy for the discussion to follow.

Discussion

Packing, conformation, and disorder

The three largest changes in structure upon desiccation (at the N-terminus, residues 66–71 and residues 87–95; Fig. 1A) are interrelated. The region near residue 89 from one molecule is in van der Waals contact with the region near residue 70 in a symmetry-related molecule, and residues 3 and 4 in a third molecule are in contact with residue 88 from the first. Also involved in this tightly packed region is the loop containing residue 38 from a fourth molecule. These residues must adjust conformation to accommodate one another in this densely packed volume. Similarly, the region near residue 113 packs between residues 43 and 122 of another molecule, which relates three more of the peaks in Figure 1A. Likewise, residue 51 and sulfate 150 are in contact with residue 23 of another molecule, in another densely packed volume (Fig. 3B). All of the larger conformational changes in Figure 1A can be accounted for in this manner. Taken together then, intermolecular packing forces are the proximate cause for the structural changes observed upon dehydration.

In the desiccated crystal structures, the ultimate source of structural change appears to be interactions with the sulfate ions. As

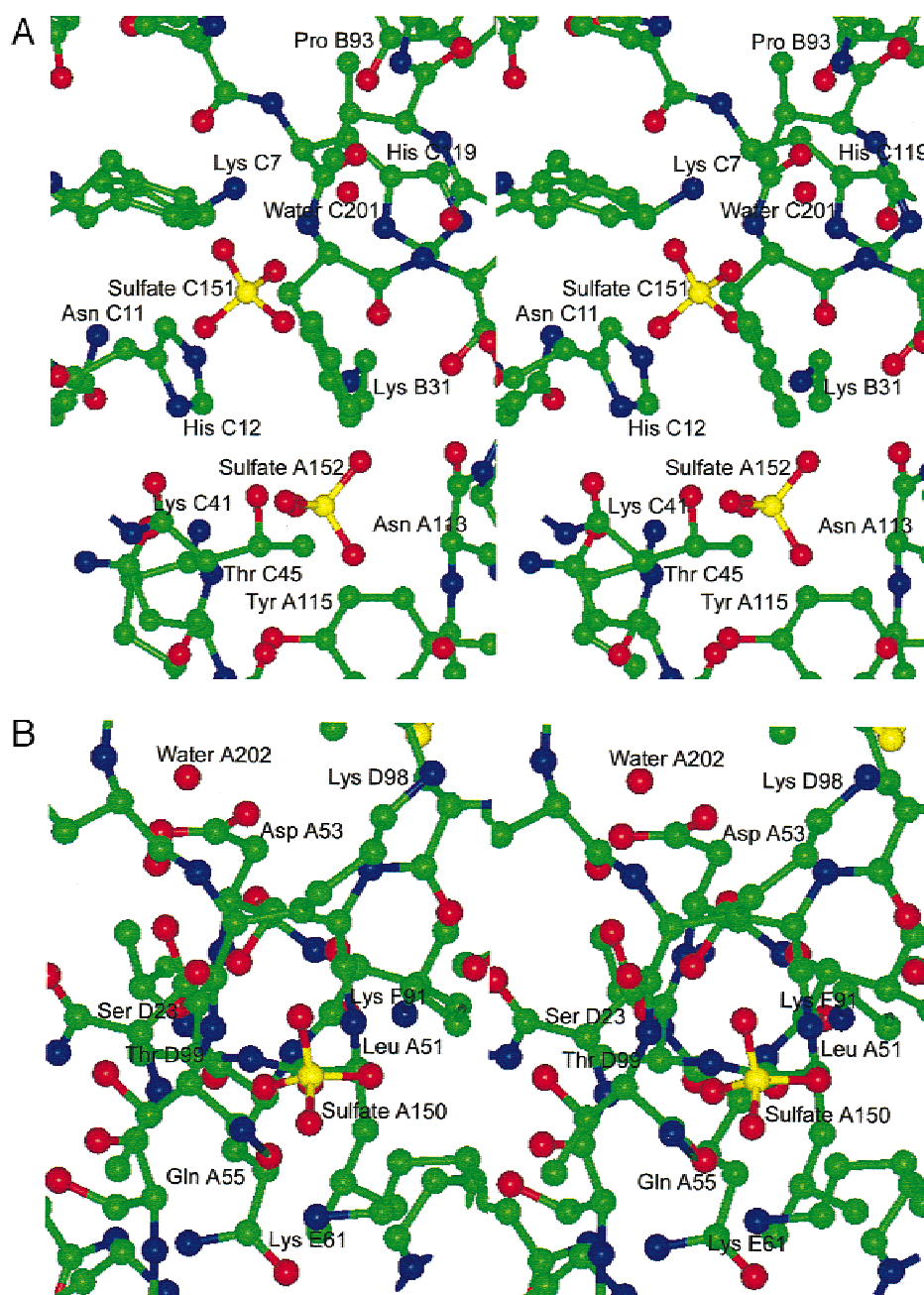


Fig. 3. Stereodiagram showing intermolecular ionic interactions involving sulfate ions, and the sites of water binding, in the 4 day desiccated crystal structure. Capital letters arbitrarily label different symmetry-related molecules in the crystal. This figure was produced with Insight II (Molecular Simulations, Inc.). **A:** The structure near sulfate ions 151 and 152 including water 201. **B:** The structure near sulfate ion 150, including water 202.

water molecules are removed, the effective dielectric constant increases and intensified electrostatic interactions drive the formation of the multiple charge-charge interactions surrounding the sulfate ions. To optimize these now very energetic ionic interactions, certain protein loops are brought into opposition. Conformational adjustments are a consequence of short van der Waals contacts that, in some regions of the protein, are relaxed by the adoption of a strained backbone conformation.

In the absence of disulfide bonds, much larger conformational changes would be anticipated. That HEWL (also a small protein

with four disulfide bonds) is the only other protein that has been successfully studied crystallographically at very low levels of hydration and without cross-linking is consistent with the importance of disulfide bonds to maintain structure under these conditions.

As solvent evaporates and additional packing interactions are introduced, residues in each unit cell do not adjust in precisely the same manner. One of several local structures may be adopted, often with strained main-chain conformations, in place of the hydrated, minimum energy structure. Absent the lubricating effect of water and especially its ability to catalyze the exchange of hydro-

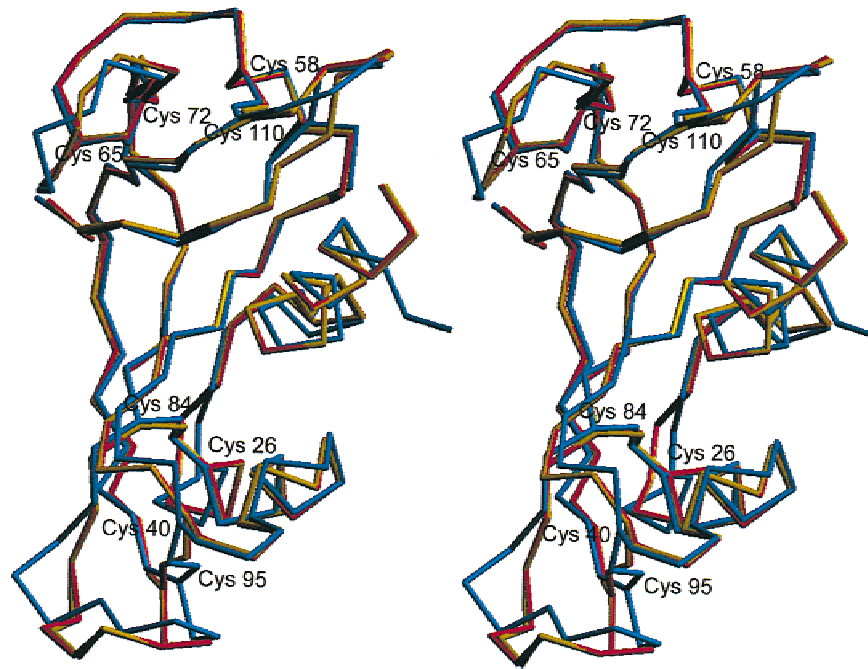


Fig. 4. Stereodiagram showing the alpha-carbon trace for ribonuclease-A after desiccation for 2.5 days (red) and 4 days (yellow), superimposed over the hydrated structure (blue). The two desiccated structures are so similar as to be almost indistinguishable in this representation. This figure was prepared using the program SETOR (Evans, 1993).

gen bonds, these conformations become kinetically trapped as they form, yielding an overall glass-like structure. This description of events leaves open the possibility of annealing the desiccated protein crystals either with sparing amounts of water or with heat.

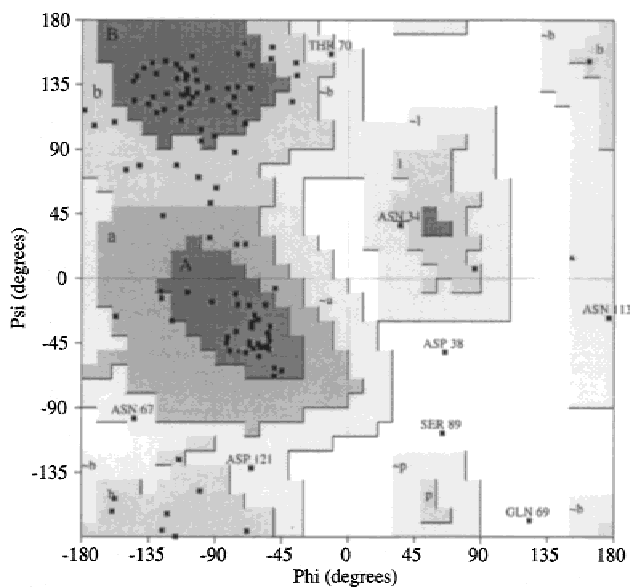


Fig. 5. Ramachandran diagram for the 2.5 day desiccated structure. Residues in unusual conformations are labeled. Asparagine 34 and aspartic acid 38 are present in similar conformations in both the hydrated (Dung & Bell, 1997) and dehydrated structures. Triangles represent glycine residues. This graph was prepared using the program PROCHECK (Morris et al., 1992).

Electrostatics, lyophilization, and molecular memory

The core of this description of protein desiccation is that optimization of electrostatic interactions drive the distortion of protein structure. In protein powders, ionic interactions would vary with different orientations of adjacent proteins, leading to many different distorted conformations. Some proteins, especially those without disulfide bonds, could be especially vulnerable to distortion, leading to the exposure of hydrophobic residues, and hence the denaturation and aggregation sometimes seen as a consequence of lyophilization. Consistent with this description of desiccation is the finding that reconstitution of lyophilized proteins is more successful if enough water is left in the sample to hydrate strongly polar groups (Hsu et al., 1992).

The structural results predict several properties of protein lyophilization. Highly charged molecules could unfold each other as they optimize electrostatic contacts, while molecules with zero net charge should tend to minimal perturbation. Thus, pH of the solution used for lyophilization could be critical to the final results. The nature and concentration of counterions should also have an effect. Since the energy of coulombic interactions is directly proportional to the charge on an ion, monovalent ions would probably introduce less perturbation in protein structure than multivalent ions.

Dehydration-related conformational effects can be explained in the context of electrostatics and counterions, but not always in a straightforward manner. For example, conformational changes in dehydrated lysozyme are not pH dependent between pH 1.9 and 5.1 with chloride as a counterion (Costantino et al., 1995). This observation is not surprising considering that this protein is strongly positively charged throughout this pH range (isoelectric point near 9.4). A more complex situation was observed with interleukin-2

(Prestrelski et al., 1995). This protein has an isoelectric point near 8. At pH 7, where net charge is small, dehydration-related conformational changes were marked, but decreased with lower pH. With greater net charge on the protein, one might expect stronger electrostatic interactions with counterions to yield larger conformational changes. Two other factors, however, are significant. First, the major counterion was 2-(N-morpholino) ethanesulfonic acid (the buffer known as MES), which has a pK_a of 6.1. These buffer molecules are converted to the zwitterionic form at low pH, which would alter the nature of counterion-mediated protein–protein interactions in the powder. Also, the increased electrostatic repulsion between the interleukin-2 molecules at lower pH may be relevant. The net effect of these two factors was less conformational change at lower pH.

An explanation for the molecular memory phenomenon follows from the above discussion. In the absence of ligand (or disulfide bonds), ionic interactions will distort the protein to such an extent as to change the binding preferences among the enzyme's possible substrates. However, a bound inhibitor could help prevent such distortion by steric interactions. The protein molecules in the powder would retain their interactions and conformations in the low dielectric environment of an organic solvent, and hence retain altered binding specificity until exposed to a high dielectric solvent once more. That dehydration-driven changes in enzyme activity are sometimes associated with conformational changes make this mechanism plausible, although it is not the only mechanism by which dehydration and organic solvents can affect enzyme activity (Griebenow & Klibanov, 1997). For conformation-related activity changes, this work provides an explanation of the connection between hydration and conformation.

Materials and methods

Crystals were grown from aqueous methanol solutions of bovine pancreatic ribonuclease A (King et al., 1962). Crystals were transferred to solutions of 95% methanol and 5% water adjusted to pH 4.5 with sulfuric acid, placed in 1 mm borosilicate capillary tubes, and blotted dry with thin strips of filter paper. All visible solvent evaporated within several minutes. Crystals were attached to the side of the capillary with a minimum amount of cyanoacrylate glue delivered to one end of the needle-shaped crystals with a glass fiber. Only the opposite end of the crystal was used for diffraction experiments. The capillaries were left open to the air for 4 days. CaSO_4 containing CoCl_2 indicator (Drierite) was powdered with mortar and pestle, and quickly packed in the base of the capillary tube, which was then sealed with wax covered with epoxy resin. The indicator did not change from its original blue color during the course of the experiments.

One data set was collected on the F-1 beamline at Cornell High Energy Synchrotron Source (CHESS), using the Princeton CCD detector (Walter et al., 1995). An R-AXIS II image plate area detector, mounted on a Rigaku RU-200 rotating anode equipped with focusing mirrors, was used for the other data set. Both experiments were performed at room temperature. The CHESS and R-AXIS crystals ($P2_12_12_1$, $a = 35.7 \text{ \AA}$, $b = 39.7 \text{ \AA}$, $c = 50.8 \text{ \AA}$) were desiccated 2.5 and 4 days, respectively, before data collection began. The CHESS data set was collected at 298 K and processed with the HKL package (Otwinowski & Minor, 1997). The R-AXIS data set was collected at 293 K, and processed with Biotex (Molecular Structure Corp., The Woodlands, Texas). Data collection

statistics are shown in Table 2. Preliminary results from this investigation have been previously reported (Bell, 1997).

The initial model for the CHESS structure was derived from molecular replacement of the fully solvated structure (Dung & Bell, 1997) using MERLOT (Fitzgerald, 1988). Two rounds of simulated annealing refinement were carried out using X-PLOR 3.1 (Brünger et al., 1987), followed by restrained least-squares refinement with TNT version 5-E, using the curvature method (Tronrud et al., 1987). Refinement of the R-AXIS data began with the simulated annealing step and proceeded independently by similar refinement methods. Residues with very high main-chain thermal factors, together with neighboring residues, were removed and rebuilt from omit maps (Bhat & Cohen, 1984) multiple times. For some stretches of amino acids, such as residues 68–71, more than 10 different models were built and evaluated during the course of refinement, in a painstaking effort to find the conformation that produced the lowest value of R_{free} . All manual adjustments to the original model were made using the program FRODO (Jones, 1985). Refinement statistics are shown in Table 2. The final five cycles of refinement included all observed reflections within the resolution limits. Structural results were validated using the programs WHAT_CHECK (Hoofst et al., 1996) and PROCHECK (Morris et al., 1992).

Table 2. Data collection and structure refinement statistics

Crystal desiccation (days)	2.5	4.0
Data collection	CHESS	R-AXIS
Resolution range, \AA	∞ to 1.9	∞ to 2.0
Wavelength, \AA	0.918	1.541
Reflections ($I/\sigma I > 1$)		
Unique observed	5,532	4,742
Total measured	38,053	14,417
Redundancy	6.5	3.0
Percent complete	91.0	84.5
R_{merge}^a	0.060	0.045
$I/\sigma I$ (% complete) by resolution		
∞ to 5 \AA	32.0 (82)	21.2 (96)
<5 to 3 \AA	38.2 (98)	14.8 (98)
<3 to 2.2 \AA	27.8 (86)	5.8 (87)
<2.2 to 2.0 \AA	—	2.5 (64)
<2.2 to 1.9 \AA	8.5 (82)	—
Refinement		
Resolution	20.0 to 1.9 \AA	10.0 to 2.0 \AA
Number of atoms	966	968
Reflections, total	5,507	4,364
Reflections, test set	541	413
R^b	0.207	0.190
R_{free}^c	0.272	0.268
Model geometry, RMSD ^c		
Bond length, \AA	0.015	0.010
Bond angle, $^\circ$	1.32	1.27
Planar groups, \AA	0.029	0.026
Trigonal atom planarity, \AA	0.008	0.008
Bad contacts, \AA (N)	0.037 (79)	0.021 (65)
B-value correlation	3.682	3.544

$$^a R_{\text{merge}} = \sum(I - \langle I \rangle) / \sum I^2.$$

^b R and $R_{\text{free}} = \sum ||F_{\text{obs}}| - |F_{\text{calc}}|| / \sum |F_{\text{obs}}|$, where R_{free} includes only amplitudes omitted from refinement working set.

^cRMSD from ideal geometry in Protgeo library (Tronrud et al., 1987).

Coordinates and structure factors for the hydrated structure (1BEL) and the dehydrated structures (1COB and 1COC) have been deposited with the Protein Data Bank.

Acknowledgments

This work was supported by a grant from the National Institutes of Health (GM50817). This work is based upon research conducted at the Cornell High Energy Synchrotron Source (CHESS), which is supported by the National Science Foundation, using the Macromolecular Diffraction at CHESS (MacCHESS) facility, which is supported by an award from the National Institutes of Health. The use of X-ray diffraction equipment of the Macromolecular Crystallographic Core Facility of the Wadsworth Center, New York State Department of Health, is gratefully acknowledged. The author thanks Patrick Van Roey for helpful discussion.

References

- Almog R, Schrier EE. 1978. The dependence of the heat of solution of lyophilized solid ribonuclease A on water content. *J Phys Chem* 82:1701–1702.
- Bell JA. 1997. The X-ray crystal structure of a highly desiccated protein. In: Ornstein RL, ed. *Biomacromolecules: From 3-D structure to applications. Proceedings 34th Hanford symposium on health and the environment*. Columbus, Ohio: Battelle. pp 231–238.
- Bhat TN, Cohen GH. 1984. Omitmap: An electron density map suitable for the examination of errors in a macromolecular model. *J Appl Cryst* 17:244–248.
- Brünger AT. 1992. Free R value: A novel statistical quantity for assessing the accuracy of crystal structures. *Nature* 355:472–475.
- Brünger AT, Kuriyan J, Karplus M. 1987. Crystallographic R factor refinement by molecular dynamics. *Science* 235:458–460.
- Carpenter JF, Pikal MJ, Chang BS, Randolph TW. 1997. Rational design of stable lyophilized protein formulations—Some advice. *Pharm Res* 14:969–975.
- Costantino HR, Griebenow K, Mishra P, Langer R, Klibanov AM. 1995. Fourier-transform infrared spectroscopy investigation of protein stability in the lyophilized form. *Biochim Biophys Acta* 1253:69–74.
- Costantino HR, Schwendeman SP, Langer R, Klibanov AM. 1998. Deterioration of lyophilized pharmaceutical proteins. *Biochemistry-Moscow* 63:357–363.
- Desai UR, Klibanov AM. 1995. Assessing the structural integrity of a lyophilized protein in organic solvents. *J Am Chem Soc* 117:3940–3945.
- Desai UR, Osterhout JJ, Klibanov AM. 1994. Protein structure in the lyophilized state: Isotope exchange/NMR study with bovine pancreatic trypsin inhibitor. *J Am Chem Soc* 116:9420–9422.
- Dong A, Meyer JD, Kendrick BS, Manning MC, Carpenter JF. 1996. Effect of secondary structure on the activity of enzymes suspended in organic solvents. *Arch Biochem Biophys* 334:406–414.
- Dung MH, Bell JA. 1997. Structure of crystal form IX of bovine pancreatic ribonuclease A. *Acta Cryst D* 53:419–425.
- Evans SV. 1993. SETOR: Hardware-lighted three-dimensional solid model representations of macromolecules. *J Mol Graphics* 11:134–138.
- Fitzgerald PMD. 1988. MERLOT—An integrated package of computer programs for the determination of crystal structures by molecular replacement. *J Appl Crystallogr* 21:273–278.
- Gregory RB, Gangoda M, Gilpin RK, Su W. 1993. The influence of hydration on the conformation of bovine serum albumin studied by solid-state ¹³C-NMR spectroscopy. *Biopolymers* 33:1871–1876.
- Griebenow K, Klibanov AM. 1995. Lyophilization-induced reversible changes in the secondary structure of proteins. *Proc Natl Acad Sci USA* 92:10969–10976.
- Griebenow K, Klibanov AM. 1997. Can conformational changes be responsible for solvent and excipient effects on the catalytic behavior of subtilisin Carlsberg in organic solvents? *Biotechnol Bioeng* 53:351–362.
- Hartsough DS, Merz KM Jr. 1992. Protein flexibility in aqueous and nonaqueous solutions. *J Am Chem Soc* 114:10113–10116.
- Hoof RWW, Vriend G, Sander C, Abola EE. 1996. Errors in protein structures. *Nature* 381:272.
- Hsu CC, Ward CA, Pearlman R, Nguyet HM, Yeung DA, Curley JG. 1992. Determining the optimum residual moisture in lyophilized protein pharmaceuticals. *Develop Biol Standard* 74:255–271.
- Jones TA. 1985. Interactive computer graphics: FRODO. *Methods Enzymol* 115:157–171.
- Kachalova GS, Morozov VN, Morozova TYa, Myachin ET, Vagin AA, Strokovyov BV, Nekrasov YuV. 1991. Comparison of the structures of dry and wet hen egg white lysozyme molecule at 1.8 Å resolution. *FEBS Lett* 284:91–94.
- King MV, Bello J, Pignataro EH, Harker D. 1962. Crystalline forms of bovine pancreatic ribonuclease. Some new modifications. *Acta Crystallogr* 15:144–147.
- Matthews BW. 1968. Solvent content of protein crystals. *J Mol Biol* 33:491–497.
- Mishra P, Griebenow K, Klibanov AM. 1996. Structural basis for the molecular memory of imprinted proteins in anhydrous media. *Biotechnol Bioeng* 52:609–614.
- Morris AL, MacArthur MW, Hutchinson EG, Thornton JM. 1992. Stereochemical quality of protein structure coordinates. *Proteins* 12:345–364.
- Nagendra HG, Sukumar N, Vijayan M. 1998. Role of water in plasticity, stability, and action of proteins: The crystal structure of lysozyme at very low levels of hydration. *Proteins* 32:229–240.
- Otwinowski Z, Minor W. 1997. Processing of X-ray diffraction data collected in oscillation mode. *Methods Enzymol* 276:307–326.
- Poole PL. 1994. The role of hydration in lysozyme structure and activity: Relevance in protein engineering and design. *J Food Eng* 22:349–365.
- Prestrelski SJ, Pikal KA, Arakawa T. 1995. Optimization of lyophilization conditions for recombinant human interleukin-2 by dried-state conformational analysis using Fourier-transform infrared spectroscopy. *Pharm Res* 12:1250–1259.
- Radha Kishan KV, Chandra NR, Sudarsanakumar C, Suguna K, Vijayan M. 1995. Water-dependent domain motion and flexibility in ribonuclease A and the invariant features of its hydration shell: An X-ray study of two low-humidity crystal forms of the enzyme. *Acta Crystallogr D* 51:703–710.
- Rupley JA, Careri G. 1991. Protein hydration and function. *Adv Protein Chem* 41:37–172.
- Shah NK, Ludescher RD. 1993. Influence of hydration on the internal dynamics of hen egg white lysozyme in the dry state. *Photochem Photobiol* 58:169–174.
- Shriver DF, Drezdson MA. 1969. *The manipulation of air-sensitive compounds*, 2nd ed. New York: Wiley-Interscience. p 72.
- Steinbach PJ, Brooks BR. 1993. Protein hydration elucidated by molecular dynamics simulation. *Proc Natl Acad Sci USA* 90:9135–9139.
- Tronrud DE. 1995. *Users' guide. The TNT refinement package*. Eugene, Oregon: Oregon State Board of Higher Education. p 34.
- Tronrud DE, Ten Eyck LF, Matthews BW. 1987. An efficient general-purpose least-squares refinement program for macromolecular structures. *Acta Crystallogr A* 43:489–503.
- Walter RL, Thiel DJ, Barna SL, Tate MW, Wall ME, Eikenberry EF, Gruner SM, Ealick SE. 1995. High-resolution macromolecular structure determination using CCD detectors and synchrotron radiation. *Structure* 3:835–844.
- Zheng YJ, Ornstein RL. 1996. Molecular dynamics of subtilisin Carlsberg in aqueous and nonaqueous solutions. *Biopolymers* 38:791–799.